Stability of nanoscale co-precipitates in a superalloy: A combined first-principles and atom probe tomography study

W. T. Geng*
School of Materials Science & Engineering and State Key Laboratory for Advanced Metals & Materials, University of Science & Technology Beijing, Beijing 100083, China

D. H. Ping,† Y. F. Gu, C. Y. Cui, and H. Harada
National Institute for Materials Science, Sengen 1-2-1, Tsukuba 305-0047, Japan

(Received 9 August 2007; revised manuscript received 22 October 2007; published 5 December 2007)

Inconel 718 is a nickel-iron based superalloy widely used in the aerospace industry. Its high temperature strength is attributed to the thermal stability of dense nanoscale precipitates γ' [Ni_3Al] and γ'' [Ni_3Nb]. There is experimental evidence that γ' and γ'' often form co-precipitates γ'/γ'' or sandwichlike structure $\gamma'/\gamma''/\gamma'$ or $\gamma''/\gamma'/\gamma''$. But how they stabilize under heat treatment or in service is still not well-understood. We have investigated the interfacial structure and chemistry of fine co-precipitates $Ni_3(Al,Ti,Nb)/Ni_3Nb(\gamma'/\gamma'')$ in Inconel 718, using both first-principles density functional theory calculation and the three-dimensional atom probe technique. Our calculations confirm that Al atoms in the γ' phase segregate to the γ'/γ'' interface. The enrichment of Al helps to impede the assimilation of Nb from γ' to γ'' and reject Al from γ'' to γ', and therefore keeps such secondary precipitates at fine size. In the absence of Ti in the γ' phase, our calculations predict an enhanced driving force for Al to accumulate at the interface. We have also characterized the microstructure of the γ'/γ'' interface for an Inconel 718 sample taken from a commercial compressor blade serviced in an airplane engine for over 10 000 h at a temperature up to 600 °C using three-dimensional atom probe analysis. Interestingly, we find that Al enrichment sustains long-term service, suggesting that the coarsening of secondary precipitates is interface-controlled. The success of first-principles density functional theory computation in reproducing the experimental observation encourages extensive application of this powerful tool in the study of precipitates in superalloys.

DOI: 10.1103/PhysRevB.76.224102 PACS number(s): 73.63.Nm, 73.22.−f

I. INTRODUCTION

Fine precipitates can usually diffuse and transform rapidly in superalloys. Very often, such small grains grow big and alter the microstructure, which in turn deteriorate the strength of the matrix material.[1] For that reason, the thermal stability of nanoscale precipitates is of particular concern in design of materials for high temperature applications. Inconel 718 is a prototype nickel-iron base superalloy containing about 5 wt % Nb along with lesser amounts of Al and Ti and also significant amounts of Cr and Mo. It was developed in the late 1960s and has since been widely used in gas turbines, rocket motors, spacecraft, nuclear reactors, pumps, and tooling due to its pronounced combination of good corrosion resistance and high strength with outstanding weldability.[2,3] An impressive fact is that Inconel 718 amounts to about 50 wt % in airplane engines.[4] Its high temperature strength is attributed to the thermal stability of dense nanoscale precipitates γ' [Ni_3Al with an ordered face-centered-cubic structure, see Fig. 1(a)] with a cubic or spherical shape and γ'' [Ni_3Nb with an ordered body-centered tetragonal crystal structure, see Fig. 1(a)] with a lenslike disk shape.[2,3,5]

The particular morphology of the precipitates and the fully coherent interfaces among the precipitates and the matrix are believed to contribute to the thermal stability.[2,3,6] In a similar alloy (Inconel 706), a three-dimensional finite element analysis has revealed that the merger of individual γ' and γ'' precipitates into γ'/γ'' co-precipitates when exposed to a service temperature of 750 °C is an energetically favorable process.[7] There is experimental evidence that γ' and γ'' often form co-precipitates γ'/γ'' or sandwichlike structure $\gamma''/\gamma'/\gamma''$ or $\gamma'/\gamma''/\gamma'$ in Inconel 718 [Fig. 1(b)].[8,9] If γ' has a cubic morphology, γ'' tends to cap the six sides of the γ' cube and forms a "compact-structure."[7] The γ'' phase is metastable and will transform to an orthorhombic δ-Ni_3Nb phase during exposure to temperature above 650 °C, resulting in a degradation of mechanical properties of this material;[10–12] but how they stabilize under heat treatment or in service is still not well-understood. For example, is the coarsening controlled by diffusion, or by interface?

The technique of three-dimensional atom probe (3DAP) tomography makes it possible to characterize atomic level structure of complex engineering materials such as superalloys.[13] With this technique one can obtain information on the size, morphology, and compositions of coexisting phases, and also the distribution of solute elements. In a beautiful work,[14] Miller has demonstrated that the crystalline orientation at the γ'/γ'' interface is $[100]_{\gamma''}\|[100]_{\gamma'}$ and $[001]_{\gamma''}\|[001]_{\gamma'}$ [Fig. 1(c)], which is in accordance with the anticipation based on lattice-match consideration. An important observation in this work is a significant Al enrichment in the γ' phase adjacent to the γ'' phase. However, the role of Al enrichment in the stabilization of co-precipitates γ'/γ'' or sandwichlike structure $\gamma''/\gamma'/\gamma''$ or $\gamma'/\gamma''/\gamma'$ is not clear. Whether it promotes or runs down the diffusion of Nb from γ' to γ'' during the coarsening process is unknown. A microscopic understanding of the thermal stability of the dual

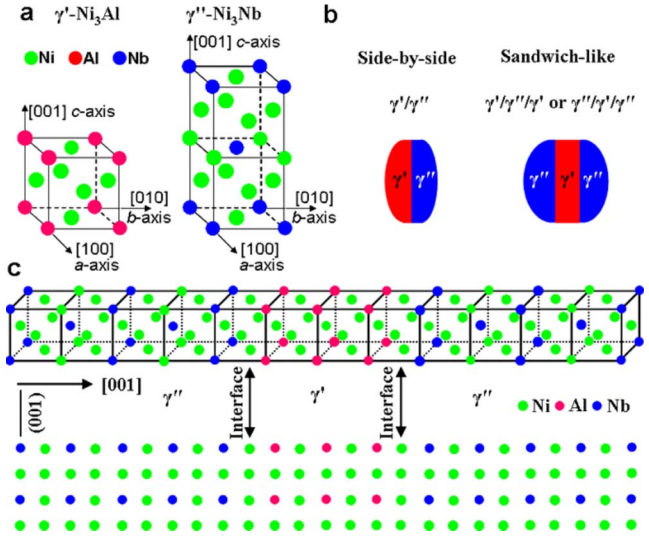

FIG. 1. (Color online) Morphology and atomic structure of γ' and γ'' nanoscale co-precipitates in Inconel 718. (a) Unit cell of γ'-Ni_3Al and γ''-Ni_3Nb. (b) Schematic drawing of the contacted co-precipitates with side-by-side (γ'/γ'') or sandwichlike ($\gamma''/\gamma'/\gamma''$ and $\gamma'/\gamma''/\gamma'$) morphology appearing in the materials. (c) Three-dimensional atomic structure of interfaces in a $\gamma''/\gamma'/\gamma''$ sandwich structure.

phase nature necessitates the detailed atomic structure at the interface. Since in 3DAP the atomic positions in the *a-b* plane are not as precisely determined as in the *c* direction, it presents a challenge to tell whether Nb atoms in γ'' phase are coplanar to the (Al, Ti, Nb) atoms in γ' phase. That is, it is hard for 3DAP to distinguish the two interfaces [Figs. 2(a) and 2(b)] that both satisfy the matching conditions $[100]_{\gamma''}\|[100]_{\gamma'}$ and $[001]_{\gamma''}\|[001]_{\gamma'}$.

The first-principles calculation method based on the density functional theory[15] is a powerful numerical weapon in determining total energy of a condensed matter system. It has been successfully applied to the study of many properties of materials directly from the fundamental equations for the electrons and it provides new insights into vital problems in not only physics and chemistry, but also materials science.[16] For instance, in the study of impurity-induced grain boundary embrittlement in alloys, first-principles calculations[17–19] have given detailed information on the energetics and chemical bonding at the grain boundary, tracing which we can understand how the cohesion across the boundary is weakened or strengthened. To our knowledge, there is yet no first-principles investigation in the study of the fine precipitates (γ' and γ'') in superalloys such as Inconel 718. This is partly due to the complexity of both the structure and composition, which makes a realistic simulation very demanding. With the continuing advances in high-performance computer development, first-principles simulation is now ready to explore the interfacial characters of co-precipitates and of precipitate-matrix in superalloys that cannot be determined by thermodynamic calculations. On the other hand, the sample used in Miller's work was laboratory-made. Although the time for isothermal aging treatments at 600 °C ranges from 10 to over 2000 h, it is still not comparable to the lifetime of a compressor blade in an airplane, which is well over 10 000 h. Thus it is of much interest to see if Al enrichment sustains the lifetime of a compressor blade.

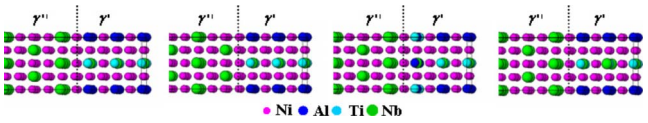

FIG. 2. (Color online) Interface of a γ'/γ'' co-precipitate subjected to the conditions $[001]_{\gamma''}\|[001]_{\gamma'}$ and $[100]_{\gamma''}\|[100]_{\gamma'}$. The magenta, lime, blue, and aqua circles represent Ni, Nb, Al, and Ti atoms. (a) An $L1_2$-type interface; (b) a DO_{22}-type interface; (c) an $L1_2$-type interface with greater Ti-Nb separation in the interfacial layer; and (d) an $L1_2$-type interface with greater Ti-Ti and Nb-Nb separation in the *a-c* plane near the γ'/γ'' interface.

In this paper, we report a combined first-principles density functional theory and three-dimensional atom probe tomography investigation of the interfacial structure and chemistry of fine co-precipitates γ'/γ'' in Inconel 718. We have employed a supercell containing 160 atoms to model the $Ni_3(Al_{0.5}Ti_{0.25}Nb_{0.25})/Ni_3Nb$ interface under matching condition $[100]_{\gamma''}\|[100]_{\gamma'}$ and $[001]_{\gamma''}\|[001]_{\gamma'}$. One difficulty encountered by first-principles methods using periodic conditions is that there is a small but non-negligible lattice mismatch in *a* (ca. 2%) between γ' and γ''. Since we have to use the same *a* for both phases in simulation of the interface, we dealt with this difficulty by examining the robustness of any conclusion with respect to the change of *a* from 3.57 Å (theoretical value for fcc Ni_3Al) to 3.64 Å (theoretical value for bct Ni_3Nb). Our total energy calculations show that at a stable γ'/γ'' interface, the interfacial Nb atoms in the γ'' phase are coplanar to the interfacial (Al, Ti, Nb) atoms in the γ' phase. We confirm the Al enrichment in the γ' phase adjacent to the γ'' phase reported by Miller[9] in a previous atom probe tomography study on a laboratory-made Inconel 718 meterial. The Al enrichment stabilizes the γ'/γ'' interface by impeding the assimilation of Nb from γ' to γ'' and rejecting Al from γ'' to γ', and therefore keeps such secondary precipitates at fine size. Moreover, our first-principles calculations predict that in the absence of Ti in the γ' phase, i.e., for a $Ni_3(Al_{0.75}Nb_{0.25})/Ni_3Nb$ interface, the driving force pushing Al to the interface will be enhanced.

Experimentally, we have investigated, using transmission electron microscopy (TEM), field ion microscopy (FIM), and 3DAP analysis, the microstructure of the γ'/γ'' co-precipitates and sandwich structures $\gamma'/\gamma''/\gamma'$ and $\gamma''/\gamma'/\gamma''$ in an Inconel 718 alloy. The samples were cut from a commercial compressor blade serviced in an airplane engine for over 10 000 h at temperatures up to 600 °C. Our measurements demonstrate that Al enrichment at the γ'/γ'' interfaces sustains long-term service and the average particle size is comparable to that found in laboratory-made materials, suggesting that the secondary precipitates are very stable in high-temperature service and their coarsening is presumably interface-controlled.

II. METHODOLOGY

The γ'/γ'' interface in question is buried in a γ matrix, which is a Ni-Cr-Fe alloy with many other additions such as

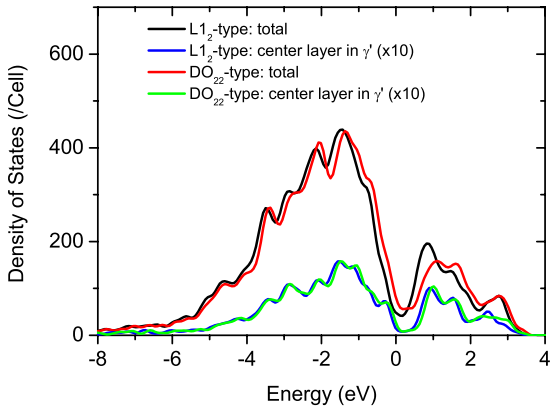

FIG. 3. (Color online) The density of states (DOS) of a γ'/γ'' co-precipitate with an $L1_2$-type or DO_{22}-type interface. Also shown are that of the center atomic layer in the γ' phase (enlarged by a factor of 10).

Mo, Ti, Nb, C, and B. The γ'/γ and γ''/γ interfaces intersect the γ'/γ'' interface at its border. Since the size of co-precipitate is from several to ten nanometers, the influence of the γ matrix on the center region of the γ'/γ'' interface will be minimal. As a result, we have chosen to treat an ideal, i.e., infinite γ'/γ'' interface in order to make the computation effort manageable. In an Inconel 718 alloy, the γ'' phase is dominantly DO_{22}-ordered Ni_3Nb.[9] As seen in Fig. 1(a), the DO_{22}-ordered structure can be viewed as an $L1_2$-ordered (Ni_3Al) structure with a $[1/2,1/2,0]$ displacement for every other (001) plane. The composition of the γ' phase, on the other hand, is rather complex. 3DAP analysis[9] showed that in the Al-containing plane of Ni_3Al lattice, a significant amount of Ti and Nb atoms sit in the Al positions, making their concentrations comparable to Al in the γ' phase. Thus we have used pure Ni_3Nb to represent the γ'' phase and adopted a partition of $Ni_3(Al_{0.5}Ti_{0.25}Nb_{0.25})$ to simulate the composition of γ'.

In a first-principles study of the γ'/γ'' co-precipitate, a difficulty we encounter when using periodic conditions is that there is a small lattice mismatch in the (001) plane (ca. 2%) between γ' and γ'' but we have to use the same lattice constant a in the (001) plane for both phases in simulation of the interface. In practice, both γ' and γ'' will change their lattice in order to match each other at the interface and will recover to their bulk values at distance. Our strategy is to adopt a single lattice a for both phases and examine the robustness of any conclusion with respect to the change of a from that of γ' (fcc Ni_3Al) to that of γ'' (bct Ni_3Nb). When we varied the lattice constant in the (001) plane, a, we have fixed the volume of the unit cell. To double the effort of computations has been time-consuming, but otherwise the final results and the conclusion drawn from that will be at risk. The unit cell to simulate the γ'/γ'' interface [see Fig. 1(c)] contains ten (001) layers of Ni_3Al and Ni_3Nb each, eight atoms (2×2 of a primary cell) in each layer and totally 160 atoms. Each phase is thick enough (about 18 Å) to mimic a realistic fine precipitate. Notice that there are identical interfaces in one unit cell, but to simulate the chemical variation of the γ'/γ'' interface we changed only one of them in order to minimize the artificial interface-interface interaction.

The first-principles density functional theory calculations were carried out using the Vienna *ab initio* simulation package (VASP).[20] The electron-ion interaction is described using the projector augmented wave method[21,22] and the exchange correlation potential using the generalized gradient approximation (GGA) in the Perdew-Burke-Ernzerhof form.[23] The energy cutoff for the plane wave basis set was 400 eV for all calculated systems. The Brillouin zone integration was performed within the Monkhorst-Pack scheme using a $(4\times4\times1)$ mesh and a Gaussian smearing of SIGMA=0.2 eV. The Ni-3d4s, Al-3s3p, Nb-4p4d5s, and Ti-3d4s electrons were treated as valence electrons. All atomic positions have been fully relaxed by minimizing the atomic forces. The optimized lattice constant for Ni_3Al is a=3.57 Å; and for DO_{22}-ordered Ni_3Nb a=3.64 Å and c=7.50 Å. Spin-polarization treatment of Ni_3Al and Ni_3Nb shows very weak magnetism. The energy difference between spin-polarized and spin unpolarized states is well below 0.01 eV per Ni_3X (X=Al,Nb), formula, and that in the optimized lattice constants is below 0.001 Å. Therefore we neglected the very weak magnetic effect in the following computations on the γ'/γ'' interfaces.

The as-received material for the present investigation is a commercial compressor blade serviced in an airplane engine. The service temperature was supposed up to 600 °C and the service time is about 10 000 h. The blade is made of Inconel 718 alloy with a nominal composition of Ni-19Fe, 21Cr, 1.8Mo, 1Al, 1Ti, 3.2Nb, 0.2C, and 0.1B in atomic percent (Ni-18.5Fe, 19Cr, 3Mo, 0.5Al, 0.9Ti, 5.1Nb, 0.04C, and 0.02B in wt %). Inconel is a trademark of the Special Metals Family of Companies. All compositions presented in this paper are given in atomic percent. Samples from the blade root

TABLE I. Energy changes (eV/cell) upon exchanging Al atoms and Ti/Nb atoms in neighboring Al-Ti-Nb layers near the $L1_2$-type γ'/γ'' interface. Numbers in parenthesis are results for a calculation cell with lattice a=3.64 Å. On the top are the concentrations of Al atoms in the interfacial Al-Ti-Nb layer in the γ' phase, and in the leftmost column are the concentrations of Ti atoms in the same layer.

Ti\\Al (%)	0%	12.5%	25%	37.5%	50%
0			0.16 (0.16)	0.02 (−0.05)	−0.13 (−0.38)
12.5		0.51 (0.60)	0.00 (0.00)	−0.04 (−0.18)	
25	0.70 (0.61)	0.30 (0.29)	−0.10 (−0.14)		

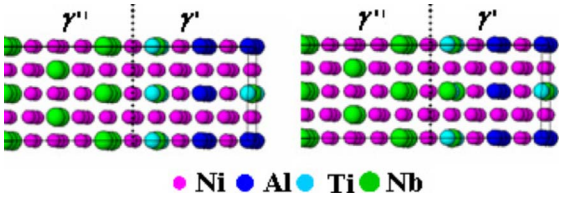

FIG. 4. (Color online) A γ'/γ'' $[Ni_3(Al_{0.5}Ti_{0.25}Nb_{0.25})/Ni_3Nb]$ interface where there is no Al atoms in the interfacial Al-Ti-Nb layer. (a) Ti-Ti and Nb-Nb nearest-neighbor distances$=a$ in the interfacial Al-Ti-Nb layer. (b) Ti-Ti and Nb-Nb nearest-neighbor distances$=\sqrt{2}\times a$.

and the different regions in the blade foil were taken for microstructural and microanalysis investigations.

Rods of approximately $0.2\times0.2\times10$ mm^3 were cut out from the blade and then electropolished first in a solution of 10% perchloric acid with 90% ethanol at room temperature and sharpened by applying microelectropolishing using an electrolyte of 2% perchloric acid in butoxyethanol for field ion microscopy (FIM) observation and three-dimensional atom probe (3DAP, Oxford nanoScience Ltd) analysis. Atom probe analyses were performed at tip temperatures of about 50 K under ultrahigh vacuum ($<1\times10^{-8}$ Pa) with a pulse fraction (a ratio of pulse voltage to the static voltage) of 0.2 and a pulse repetition rate of 1500 Hz. A JEOL high resolution TEM (JEM 4000EX) operated at 400 kV was also used for observing the fine precipitate morphology. Thin foils for TEM observations were prepared by means of a standard twinjet polishing technique in a solution of 23% perchloric acid and 77% acetic acid at about −30 °C.

III. RESULTS AND DISCUSSION

A. Computation

1. Interfacial structure prior to atomic segregation

There are two possible configurations for an ideal $Ni_3(Al_{0.5}Ti_{0.25}Nb_{0.25})/Ni_3Nb$ $[\gamma'/\gamma'']$ contact subjected to the conditions $(001)_{\gamma''}\|(001)_{\gamma'}$ and $(100)_{\gamma''}\|(100)_{\gamma'}$, as shown in Figs. 2(a) and 2(b). By "ideal" we mean there is no atomic segregation on either side of the interface. We denote them as $L1_2$-type interface and DO_{22}-type interface, respectively. For simplicity in presentation, we denote the all-Ni layer as A layer, the Nb-containing layer in the γ'' phase as B layer, and the Al-containing layer in the γ' phase as C layer.

Our total energy calculations demonstrate that when γ'' was forced to match γ' in the (001) plane (a=3.57 Å), the $L1_2$-type interface is 0.45 eV/(eight interfacial Ni atoms), i.e., 0.14 J/m^2, more stable than the DO_{22}-type interface; whereas when γ' was forced to match γ'' in the (001) plane (a=3.64 Å), it is 0.52 eV (0.16 J/m^2) more stable than the latter. We then conclude that the $L1_2$-type interface structure is more stable than the DO_{22}-type interface. To understand this preference, we have compared the total energy of an ordered alloy $Ni_3(Al_{0.5}Nb_{0.5})$ with an $L1_2$-like or a DO_{22}-like alignment. Our calculation shows that the $L1_2$ structure is 0.66 eV (per Ni_6AlNb formula) lower in energy than the

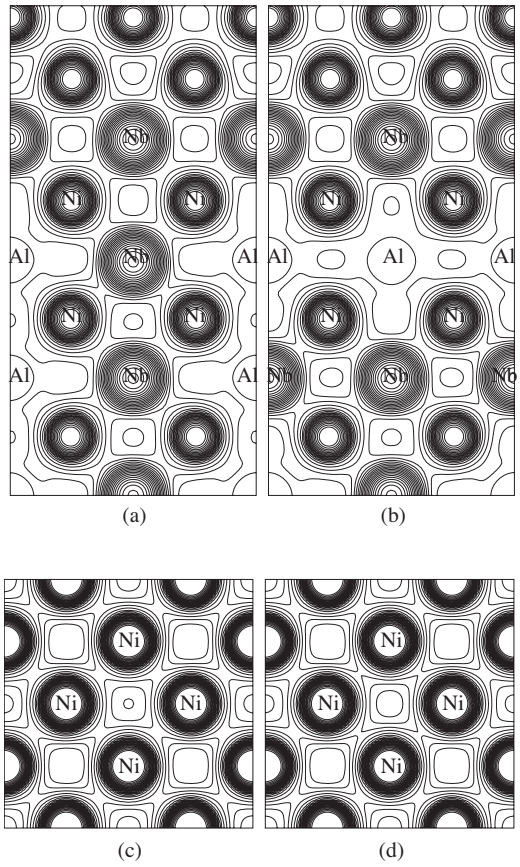

FIG. 5. The calculated valence charge density near the γ'/γ'' interface, with [panels (b) and (d)] and without interfacial Al enrichment [panels (a) and (c)]. Panels (a) and (b) display the charge density in the (100) plane; panels (c) and (d) are for the interfacial Ni plane [(001)]. Contours start from 0.2 e/Å^3 and increase successively by a factor of $2^{1/4}$.

DO_{22} structure. This indicates that Al and Nb atoms separated by a Ni plane tend to be coplanar, which explains the stability of the $L1_2$-type γ'/γ'' interface.

We show in Fig. 3 the calculated density of states (DOS) of both the whole system and the center atomic layer in the γ' phase (comprising four Ni, two Al, one Nb, and one Ti atoms in the unit cell), with either an $L1_2$-type or DO_{22}-type interface. It is seen clearly that the electronic states near the Fermi level have lower energy in the case of the $L1_2$-type γ'/γ'' interface; whereas the DOS of the center layer in the γ' phase is hardly changed. As a result, the co-precipitate with an $L1_2$-type interface is energetically favorable.

We note that the distribution of Ti and Nb in the γ' phase is possibly random. At the interface, however, there might be some preference in the Ti-Nb positioning. We have compared the total energy of the structures shown in Fig. 1(a) and that in Fig. 1(c). For the calculation cell with a=3.57 Å we find that the former configuration ($d_{\text{Ti-Nb}}=a$) is 0.21 eV lower in energy that the latter case ($d_{\text{Ti-Nb}}=\sqrt{2}\times a$); and for the cell with a=3.64 Å, the energy lowering is 0.20 eV. It can then be concluded that Ti and Nb tend to sit close to each other in the interfacial C layer. In addition, we examined the preferred Ti/Ti (Nb-Nb) distance between interfacial and subinterfacial C layers. In the configuration shown in Fig. 1(a),

TABLE II. Same as Table I, but for the DO_{22}-type interface.

Ti\\Al (%)	0%	12.5%	25%	37.5%	50%
0			−0.10 (−0.09)	0.38 (0.30)	0.93 (0.71)
12.5		−0.02 (−0.09)	0.00 (0.00)	0.60 (0.47)	
25	−0.09 (−0.27)	0.01 (−0.03)	0.17 (0.14)		

the nearest Ti/Ti and Nb-Nb distance is a; and in Fig. 1(d) it is $\sqrt{2}\times a$. When $a=3.57$ Å the former alignment is only 0.01 eV lower in energy than the latter; and when $a=3.64$ Å, it is also only 0.01 eV more stable. These two configurations are therefore energetically degenerated.

2. Al segregation in γ'

The Al enrichment in the γ' region adjacent to the γ'' phase occurs if Al segregates from the inner part of the γ' region to the γ'/γ'' interface, and/or, if Nb atoms are attracted out from γ' and Al atoms are rejected from the γ'' phase during coarsening of the secondary precipitates.[9] In this section, we study the first process. In the computational cell we set up, we model the Al segregation from the inner part of γ' by exchanging Al atoms in the subinterfacial C layer and Nb/Ti in the interfacial C layer. To make the computation affordable, we have refrained ourselves from examining segregation involving more layers. This approximation is reasonable in view of the fact that (i) in general cases remarkable segregation will occur in only a handful of layers near the surface or interface and (ii) Al enrichment was found only in the interfacial C layer in experiment.[9] Since there are eight atoms (four are Ni) in the (001) plane of the unit cell, the Al concentration in the interfacial C layer can be 0%, 12.5%, 25%, 37.5%, and 50%. More continuous distributions in either the (001) plane or along the c direction will make the unit cell used to simulate the interface too large and hence the computation too demanding.

The presence of Ti introduces complexity of the interfacial structure/chemistry. Each time we vary the Al concentration in the interfacial C layer (that for the subinterfacial C layer will change accordingly), we need to consider both Al-for-Ti and Al-for-Nb cases. We note that the two Al atoms in a C layer are not equivalent, with one sitting close to Ti and the other to Nb [see Fig. 1(a)]. When we exchanged Al with Ti/Nb from a neighboring C layer, we assumed the shorter path ($d=\sqrt{2}\times a$) is preferred to the longer one ($d=\sqrt{3}\times a$).

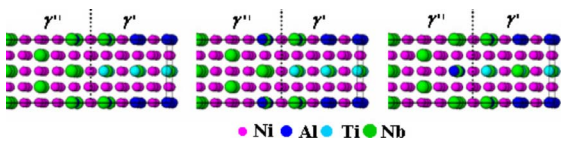

FIG. 6. (Color online) A γ'/γ'' [$Ni_3(Al_{0.5}Ti_{0.25}Nb_{0.25})/Ni_3Nb$] interface where some Al atoms in the interfacial Al-Ti-Nb layer penetrate into the interfacial Nb layer in the γ'' phase, with a nearest-neighbor Al-Al distance $d_{Al\text{-}Al}=a$ (left), $\sqrt{2}\times a$ (center), or $\sqrt{3}\times a$ (right) across the interface.

The calculated energy changes (in eV/cell) upon exchanging Al atoms and Ti/Nb atoms in neighboring C layers near the γ'/γ'' interface are listed in Table I. The top line gives the concentrations of Al atoms in the interfacial C layer in the γ' phase, and the leftmost column lists the concentration of Ti atoms in the same layer. Results for both $a=3.57$ and 3.64 Å (numbers in parenthesis) are presented. Two trends are clearly seen in this table. First, the system gets more stable when Al atoms in the subinterfacial C layer diffuse into the interfacial C layer (with Ti or Nb atoms moving reversely) and less stable vise versa. Second, we notice that Ti accumulation at the interface also helps stabilize the co-precipitates. Also, it is impressive that the calculation cells with $a=3.57$ and 3.64 Å yield quantitatively the same results. Hence we are confident with the first-principles computations, which confirm the Al enrichment previously observed in experiment.[9] We stress that the segregation of Al to the γ'/γ'' interface in such a complex system cannot be predicted by simple thermodynamics.

Note that when there are no Al atoms in the interfacial layer, i.e., Ti-25% and Nb-25%, an ordered distribution will give a Ti-Ti (Nb-Nb) distance of either a or $\sqrt{2}\times a$ [see Figs. 4(a) and 4(b)]. For $a=3.57$ Å, calculations show that these two alignments are almost energetically degenerated, with the former only 0.01 eV more stable than the latter. And for $a=3.64$ Å, the small separation case is 0.02 eV more stable.

To gain some insight into the underlying physics of Al enrichment at the γ'/γ'' interface, it is necessary to study the change in electronic structure of the interface upon segregation of Al. In Fig. 5, we display the calculated valence charge density ($e/\text{Å}^3$) near the γ'/γ'' interface, with [panels (b) and (d)] and without interfacial Al enrichment [panels (a) and (c)]. Panel (a) and (b) display the charge density in the (100) plane; panels (c) and (d) are for the interfacial Ni plane [(001)]. To simulate Al segregation, we exchange one Al atom in the subinterfacial Al-containing layer with the Nb atom in the interfacial Al-containing layer. Thus the (100) plane we chose is the one containing Nb atoms. It is shown in Fig. 5 that exchanging atoms between different layers gives rise to perturbation of valence electron distribution only around the involved atomic layers. A comparison of panels (a) and (b) tells us that the accumulation of Al atoms at the interface results in an increase in the valence charge density in the region between the interfacial Ni layer and Al-containing layer, an indication of a somewhat strengthening of the chemical bonding between these two atomic layers. On the other hand, we see clearly from panels (c) and (d) that the accumulation of Al atoms at the interface reduces the valence charge density in the very center region of the interfacial Ni layer, suggesting that the intralayer bonding be-

TABLE III. Energy changes (eV/cell) upon exchanging Al atoms and Nb atoms across the γ'/γ'' interface.

$d_{\text{Al-Al}}$	a	$\sqrt{2}\times a$	$\sqrt{3}\times a$
ΔE (a=3.57 Å)	0.17	0.35	0.23
ΔE (a=3.64 Å)	0.18	0.36	0.22

tween Ni atoms is slightly weakened. The combined effect lowers the total energy of the whole system.

3. Rejection of Al from the γ'' phase

To model the repelling of Al from the γ'' phase into the γ' region and simultaneously attracting Nb from the γ' region across the interface, we need a γ'' phase containing Al. Experiment evidenced that the content of Al in γ'' is very low, and hence a realistic simulation of Al-in-γ'' requires a huge periodic cell and therefore is computationally too demanding. It is reasonable, nevertheless, to involve Al atoms only in the interfacial B layer in γ'' and examine the movement of Al. Interestingly, with Al in the interfacial B layer in γ'', this layer can be viewed as the interfacial C layer in γ'; and the interface structure is not an $L1_2$-type, but rather a DO_{22}-type interface [see Figs. 2(a) and 2(b)]. Then, the question becomes: How will a DO_{22}-type γ'/γ'' interface evolve?

Following the same way we treated the $L1_2$-type interface, we calculated the energy changes (in eV/cell) upon exchanging Al atoms and Ti/Nb atoms in neighboring C layers near the DO_{22}-type γ'/γ'' interface. The results are listed in Table II. The top line gives the concentrations of Al atoms in the interfacial C layer in the γ' phase, and the leftmost column lists the concentration of Ti atoms in the same layer. Results for both a=3.57 and 3.64 Å (numbers in parenthesis) are presented. Contrary to the case of $L1_2$-type interface, the concentration of Al in the interfacial C layer tends to decrease and Nb atoms underneath will segregate to the interface simultaneously. The lowest energy state was reached when all the Al atoms were substituted by Nb. Interestingly, the interfacial C layer in the γ' phase then becomes the interfacial B layer in γ''. Meanwhile, the interface transforms from DO_{22}-type to $L1_2$-type and Al in γ' starts to accumulate at the interface.

4. Penetration of Al into γ'

It is well-established in experimental work that Al atoms will move only from γ'' to γ', but not vice versa. We examine this process by evaluating the energy change of the coprecipitate when exchanging the interfacial Al atoms in the $Ni_3(Al_{0.5}Ti_{0.25}Nb_{0.25})$ phase with the interfacial Nb atoms in the Ni_3Nb region. For the simulation model we adopted, there are eight configurations corresponding to such an Al-Nb exchange, two with a nearest-neighbor Al-Al distance $d_{\text{Al-Al}}=a$ across the interface, four with $d_{\text{Al-Al}}=\sqrt{2}\times a$, and another two with $d_{\text{Al-Al}}=\sqrt{3}\times a$. Three of these eight configurations, one with $d_{\text{Al-Al}}=a$ (left), one with $d_{\text{Al-Al}}=\sqrt{2}\times a$ (center), and one with $d_{\text{Al-Al}}=\sqrt{3}\times a$ (right) are sketched in Fig. 6.

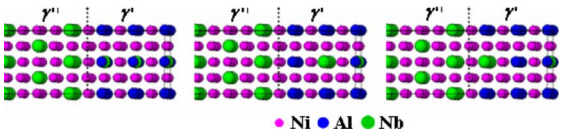

FIG. 7. (Color online) A γ'/γ'' [$Ni_3(Al_{0.75}Nb_{0.25})/Ni_3Nb$] interface in the absence of Ti. The Al concentration in the interfacial Al-Nb layer is (left) 37.5%, (center) 50%, and (right) 25%.

The calculated total energies for the three configurations depicted in Fig. 6, in reference to that of the sharp γ'/γ'' interface are tabulated in Table III. It is clear that for both a=3.57 and 3.64 Å cases, Al atoms across the interface tend to sit close to each other, but still, this is not energetically favorable compared with the sharp interface. As a result, Al atoms in the γ' region in adjacent to the γ'' phase will not penetrate into the latter region.

5. Role of Ti

Prompted by the discovery that Ti atoms in the γ' phase tend to accumulate at the γ'/γ'' interface, we have performed computations to examine the effect of Ti on Al enrichment. In the computation cell to model the γ'/γ'' co-precipitate, we replaced Ti in γ' with Al. So, now we have a system of $Ni_3(Al_{0.75}Nb_{0.25})/Ni_3Nb$ [see Fig. 7(a)]. Similar to the case with Ti, we vary the Al concentration in the interfacial C layer by exchanging Al and Nb atoms between the interfacial and subinterfacial C layers. Figures 7(b) and 7(c) are the sketched interfaces with an Al concentration of 50% and 25%. We know from above investigations that Al atoms in the interfacial C layer tend to stay close to each other; it is reasonable to expect the same phenomena in the absence of Ti. Therefore we explored only one configuration for Al-25% and Al-50% cases.

Table IV displays the numerical results given by first-principles calculations. We see that in the absence of Ti, Al atoms still have a tendency to accumulate at the γ'/γ'' interface. Furthermore, a comparison of the energy changes with those in the case when Ti is present in γ' (cf. Table I) indicates that the force driving Al to the interface gets stronger when Ti atoms are replaced by Al. For example, when an Al atom (in a unit cell) goes from the subinterfacial C layer for a Nb atom in the interfacial C layer, the energy lowering is 0.04 eV with Ti and 0.23 eV without Ti, for the lattice constant a=3.57 Å. When a=3.64 Å is employed, the energy lowering is 0.18 eV with Ti and 0.32 eV without Ti.

We plot in Fig. 8 the calculated valence charge density ($e/\text{Å}^3$) near the γ'/γ'' interface, with [panels (b) and (d)] and without interfacial Al enrichment [panels (a) and (c)]. Panels

TABLE IV. Energy changes (eV/cell) upon exchanging Al atoms and Nb atoms in neighboring Al-Nb layers near the γ'/γ'' interface. Numbers in parenthesis are results for a calculation cell with lattice a=3.64 Å. On the top are the concentrations of Al atoms in the interfacial Al-Nb layer in the γ' phase. Numbers in parenthesis are that for Nb in the same layer.

Al (Nb) content	25% (25%)	37.5% (12.5%)	50% (0.0%)
ΔE	0.47 (0.41)	0.00 (0.00)	−0.23 (−0.32)

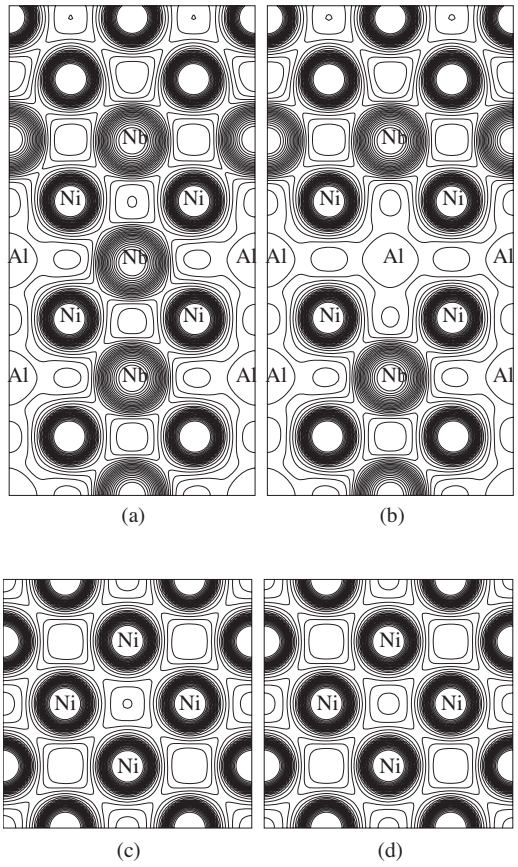

FIG. 8. Same as Fig. 5, but for the case when Ti is replaced by Al throughout the γ' phase. The γ' phase has the formula $(Ni_3Al_{0.75}Nb_{0.25})$.

(a) and (b) display the charge density in the (100) plane; panels (c) and (d) are for the interfacial Ni plane [(001)]. Figure 8 shows quite similar features as Fig. 5. In the absence of Ti, Al enrichment again increase the valence charge density in the region between the interfacial Ni layer and Al-containing layer, hence a somewhat strengthening of the chemical bonding between these two atomic layers. Similarly, panels (c) and (d) show that the accumulation of Al atoms at the interface reduces the valence charge density in the very center region of the interfacial Ni layer, an indication that the intralayer bonding between Ni atoms is slightly weakened. Altogether, the charge redistribution lowers the total energy of the whole system.

6. Distribution of Ni

Finally, we made an attempt to elucidate the state of Ni, the majority element in superalloy Inconel 718. From the ideal $L1_2$-type γ'/γ'' interface [Fig. 2(a)], we exchanged positions of Al in the subinterfacial (or interfacial) C layer with Ni in the interfacial (or subinterfacial) C layer to get an Al content of 37.5% or 12.5% in the interfacial C layer. Our first-principles calculations for both cases yield a total energy increase over 2 eV. Electronic structure analysis shows that below the Fermi level the DOS (not shown) for the relocated Ni atom increases greatly, which makes its bonding state unstable. On the other hand, the states of Al experience a much smaller change. This means that Ni atoms are not involved in the atomic redistribution in the aging of precipitates.

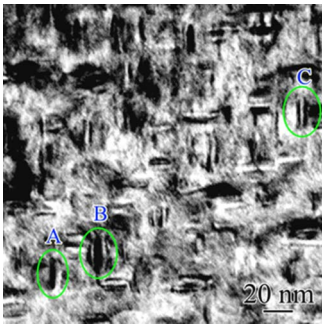

FIG. 9. (Color online) A typical transmission electron microscope photograph for a commercial compressor blade serviced for a long period in an airplane engine. The blade is made of Inconel 718 alloy. The precipitates with dark contrast correspond to γ''-Ni_3Nb as Nb is heavier than Al. The co-precipitates γ'/γ'' (A region), sandwichlike $\gamma'/\gamma''/\gamma'$ (B region), and $\gamma''/\gamma'/\gamma''$ (C region) morphology are clearly seen.

B. Experiment

Figure 9 is a typical transmission electron microscope (TEM) photograph taken of a commercial compressor blade (made of Inconel 718) serviced in an airplane engine for a long period (total flight time is over 10 000 h). The sandwichlike [$\gamma'/\gamma''/\gamma'$ (B region) or $\gamma''/\gamma'/\gamma''$ (C region)] and co-precipitates [γ'/γ'' (A region)] morphology is commonly observed. The precipitates with a dark contrast are γ'' since it contains Nb, which is a heavier element than Al; γ' shows a weak contrast when observed in a TEM bright field mode. The average size (the diameter of the disk-shaped or platelike precipitates) of both γ' and γ'' precipitates is about 20 nm. We have no way to check the microstructure in the same sample before service. However, compared with the average particle size in a commercial Inconel 718 material heat-treated in the standard conditions,[24] no significant coarsening can be noticed in the present investigation. In fact, an extraordinary long thermal exposure (50 000 h) has been carried out on this kind of materials at 593 °C, mechanical properties and microstructures have shown only subtle changes, which further illustrate the excellent stability.[25,26]

The coarsening behaviors of the nanoscale γ' and γ'' precipitates in Inconel 718 has been investigated in detail in a temperature range of 700–750 °C, and it was suggested that the coarsening kinetics of both γ' and γ'' follow a Lifshitz-Slyozov-Wagner (LSW) theory of bulk diffusion-controlled precipitate coarsening, which means that the grain size difference has a $d_t^3 - d_0^3 \sim t$ relationship with the aging time (d_t is an average particle diameter after the material is aged for time t; d_0 is the initial average diameter prior to aging).[27] Strictly speaking, the LSW theory is applicable to isolated spherical particles. The role of the γ'/γ'' interfaces on the thermal stability of the nanoscale precipitates should not be ignored since the γ' and γ'' nanoscale precipitates always

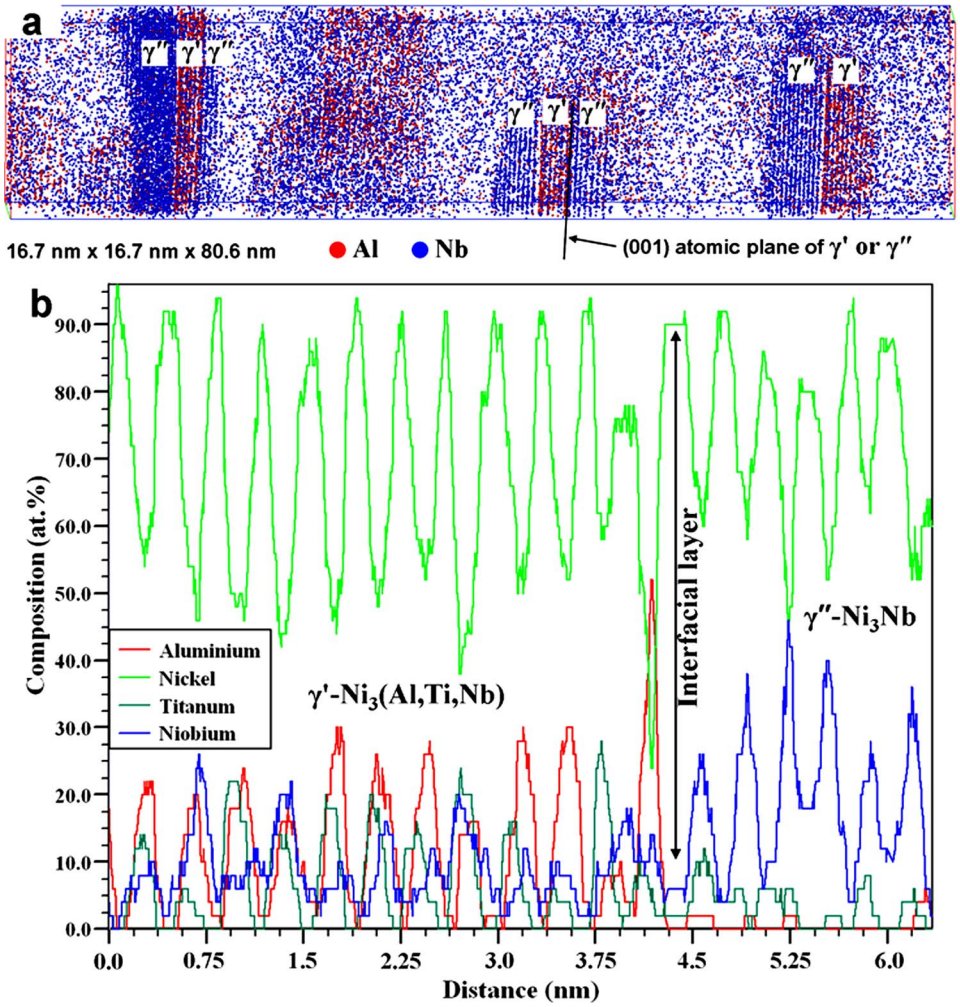

FIG. 10. (Color online) 3D atomic distributions at a γ'/γ'' interface. (a) Elemental mappings of Al and Nb atoms in an analyzed volume of $16.7\times16.7\times80.6$ nm^3, which contains several γ' and γ'' precipitates. The morphology of the precipitates is quite close to that shown in Fig. 1(b) and the average precipitate size is about 20 nm. The (001) atomic planes of both γ' and γ'' phases are clearly imaged and the γ'/γ'' interfaces are sharp at an atomic scale. (b) Chemical concentration depth profiles along the c axis. Al enrichment is remarkable in the interfacial (001) layer in the γ' side.

occur in the co-precipitates structure in Inconel 718 and other similar alloys. In the present investigation, three-dimensional atom distribution of various alloying elements at the γ'/γ'' interfaces in the compressor blade made of Inconel 718 after service in an airplane engine has been realized by means of the three-dimensional atom probe (3DAP) technique, which has an ultimate depth resolution of one atomic scale, and is able to map out both chemical composition and atoms in three dimensions.[28,29]

The morphology and chemical composition of the nanoscale γ' and γ'' precipitates can be virtually observed in three-dimensions. Figure 10(a) is a three-dimensional atom mapping of Al and Nb elements in an analyzed volume of $16.7\times16.7\times80.6$ nm^3. Each dot corresponds to one atom in the map. The (001) atomic planes of γ' or γ'' are clearly visible. The Al-rich region is γ' phase and the Al-poor area corresponds to γ'' phase. The γ'/γ'' interface is atomically smooth or sharp. The selected volume did not include $\gamma'/\gamma''/\gamma'$ structure, but the three kinds of structures (γ'/γ'', $\gamma'/\gamma''/\gamma'$, and $\gamma''/\gamma'/\gamma''$) seemed to be equally observed. One of the γ'/γ'' interfaces was selected and the layer-by-layer concentration profiles of Ni, Al, Ti, and Nb elements at (001) planes has been quantitatively analyzed [Fig. 10(b)]. We notice that Nb atoms are also partitioned in the γ' phase with an average amount of 15 at. % and distributed in the Ni-Al-Ti layers. Thus the present γ' phase is $Ni_3(Al,Ti,Nb)$, one (001) atomic plane is compose mostly by Ni (with a small amount of Fe and Cr atoms), the next is the Ni-Al-Ti-Nb layer. In the γ'' phase, the Ni-Nb layers contain only a very small amount of Ti and nearly no Al. We note that the content of Nb was underestimated with respect to Ni as it is heavier than the latter and hence has a much lower evaporating rate in the electric field. Impressively, Al is found to be enriched in the interfacial layer in the γ' side. To make sure this enrichment is not an artifact, we have performed full measurement on the chemical concentration depth profiles of a $\gamma''/\gamma'/\gamma''$ sandwichlike structure. The data are plotted in Fig. 11. Strikingly, Al enrichment appears at both γ''/γ' and γ'/γ'' interfaces. This scrutiny rules out the possibility of an artificial Al enrichment caused by a particular choice of probing direc-

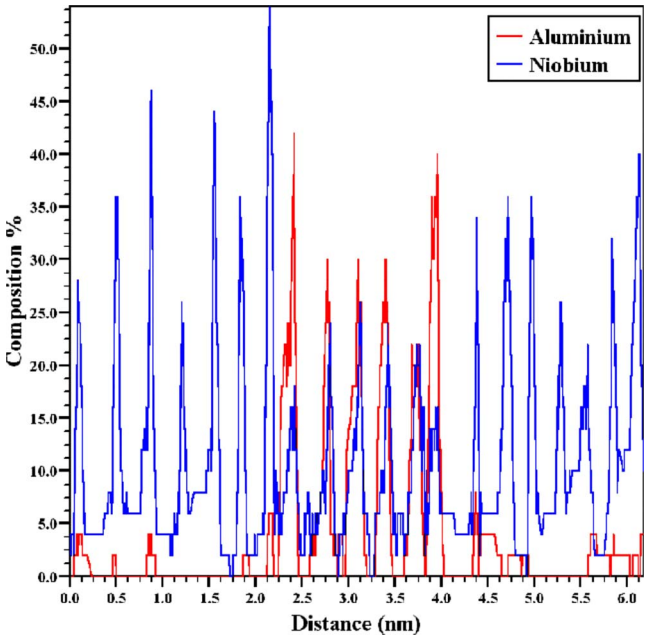

FIG. 11. (Color online) Chemical concentration depth profiles of a $\gamma''/\gamma'/\gamma''$ sandwichlike structure. Al enrichment appears at both γ''/γ' and γ'/γ'' interfaces. This result means that the enrichment is not an artifact from the different probing directions in the 3DAP.

tion in the 3DAP. Our measurements support Miller's view that during the coarsening of the γ'' precipitates, the Al atoms are rejected from the γ'' region and partitioned into the γ' phase, finally the Al atoms piled up at the atomic layer next to the Ni interfacial layer. Meanwhile, the Al enriched layer serves as a barrier for the diffusion of the Nb atoms from γ' into the γ'' phase, which hinders the grain growth of the γ'' phase.

IV. SUMMARY

To summarize, we have carried out both a first-principles density functional theory and a three-dimensional atom probe tomography study on the interfacial structure and chemistry of the γ'/γ'' co-precipitates in superalloy Inconel 718. The first-principles calculations prove to be able to offer detailed information on the structure and chemistry of the interface, which are not readily available from thermodynamics. We have revealed that the diffusion of Nb across the γ'/γ'' interfaces is energetically unfavorable, which means that an interface-controlled coarsening is likely a predominant kinetic while the precipitates formed co-precipitates. In addition to the confirmation of previous observations such as Al enrichment at the interface, we also predict that in the absence of Ti, the driving force pushing Al in the γ' region to the interface will be strengthened. This prediction calls for experimental verification. We expect this work to encourage more computational efforts in the study of precipitates in superalloys.

Using three-dimensional atom probe analyses on a commercial blade, we have observed Al enrichment at the γ'/γ'' interface in the γ' side. Our measurements show that the average particle size is comparable to that in a laboratory-made material. As the Al enrichment at the γ'/γ'' interfaces sustains long-term service, it is suggestive that the secondary precipitates are very stable in high-temperature service.

ACKNOWLEDGMENTS

The work in China was supported by the National Natural Science Foundation of China under Grant No. 50671011 and the NCET.

*Author to whom correspondence regarding theory should be addressed. geng@mater.ustb.edu.cn

†Author to whom correspondence regarding experiments should be addressed. ping.de-hai@nims.go.jp

[1] D. A. Porter and K. E. Easterling, *Phase Transformations in Metals and Alloys*, 2nd ed. (Chapman & Hall, London, 1992).

[2] C. T. Sims, N. S. Stoloff, and W. C. Hagel, *Superalloys II* (Wiley, New York, 1987).

[3] E. A. Loria, *Superalloys 718, 625, 706 and Various Derivatives* (TMS-The Minerals, Metals & Materials Society, Warrendale, 2005).

[4] R. E. Schafrik, D. D. Ward, and J. R. Groh, in *Superalloys 718, 625, 706 and Various Derivatives*, edited by E. A. Loria (TMS-The Minerals, Metals & Materials Society, Warrendale, 2001), pp. 1–11.

[5] W. E. Quist, R. Taggart, and D. H. Polonis, Metall. Trans. **2**, 825 (1971).

[6] C. T. Sim and W. C. Hagel, *The Superalloys* (Wiley, New York, 1972).

[7] V. Kindrachuk, N. Wanderka, and J. Banhart, Mater. Sci. Eng., A **417**, 82 (2006).

[8] D. F. Paulonis, J. M. Oblak, and D. S. Duvall, Trans. ASM **62**, 611 (1969).

[9] R. Cozar and A. Pineau, Metall. Trans. **4**, 47 (1973).

[10] J. F. Barker, E. W. Ross, and J. F. Radavich, J. Met. **22**, 31 (1970).

[11] M. Sundararaman, P. Mukhopadhyay, and S. Banerjee, Metall. Trans. A **19A**, 453 (1988).

[12] J. He, G. Han, S. Fukuyama, and K. Yokogawa, Acta Mater. **46**, 215 (1998).

[13] M. K. Miller, *Atom Probe Tomography: Analysis at the Atomic Level* (Kluwer Academic/Plenum, New York, 2000).

[14] M. K. Miller, Micron **32**, 757 (2001).

[15] P. Hohenberg and W. Kohn, Phys. Rev. **136**, B864 (1964); W. Kohn and L. J. Sham, Phys. Rev. **140**, A1133 (1965).

[16] R. M. Martin, *Electronic Structure: Basic Theory and Practical Methods* (Cambridge University Press, Cambridge, England, 2004).

[17] R. Wu, A. J. Freeman, and G. B. Olson, Science **265**, 376 (1994).

[18] M. Yamaguchi, M. Shiga, and H. Kaburaki, Science **307**, 393

(2005).
[19] W. T. Geng, J. S. Wang, and G. B. Olson, Science **309**, 1677c (2005)/10.1126/science.1112072.
[20] G. Kresse and J. Furthmüller, Phys. Rev. B **54**, 11169 (1996); Comput. Mater. Sci. **6**, 15 (1996).
[21] P. E. Blochl, Phys. Rev. B **50**, 17953 (1994).
[22] G. Kresse and D. Joubert, Phys. Rev. B **59**, 1758 (1999).
[23] J. P. Perdew, K. Burke, and M. Ernzerhof, Phys. Rev. Lett. **77**, 3865 (1996).
[24] M. K. Miller, S. S. Babu, and M. G. Burke, Mater. Sci. Eng., A **327**, 84 (2002).
[25] G. E. Korth and C. L. Trybus, in *Superalloys 718, 625 and Various Derivatives*, edited by E. A. Loria (TMS-The Minerals, Metals & Materials Society, Warrendale, 1991), pp. 437–446.
[26] S. Mannan, S. Patel, and J. Debarbadillo, in *Superalloys 2000*, edited by T. M. Pollock, R. D. Kissinger, R. R. Bowman, K. A. Green, M. McLean, S. Olson, and J. J. Schirra (TMS-The Minerals, Metals & Materials Society, Warrendale, 2000), pp. 449–458.
[27] Y. F. Han, P. Deb, and M. C. Chaturvedi, Met. Sci. **16**, 555 (1982).
[28] D. Blavette, B. Deconihout, S. Chambreland, and A. Bostel, Ultramicroscopy **70**, 115 (1998).
[29] M. K. Miller and G. D. W. Smith, *Atom Probe Microanalysis: Principles and Applications to Materials Problems* (MRS-Materials Research Society, Pittsburgh, 1989).